Dynamic Mode Decomposition in Various Power System Applications

Abdullah Alassaf
Electrical Engineering Department
University of South Florida,
Tampa, FL 33620, USA
University of Hail, Hail, KSA
Email: alassaf@mail.usf.edu

Lingling Fan
Electrical Engineering Department
University of South Florida,
Tampa, FL 33620, USA
Email: linglingfan@usf.edu

***Abstract*—Due to the complexity of modeling the actual dynamic large-scale power system, free-equation model identification techniques have been found more practical. Recently, Dynamic Mode Decomposition (DMD) has been proposed and used in fluid dynamics and brain modeling. In power systems, DMD applications just kick off. This paper reviews the DMD algorithm and implements DMD for mode identification and signal reconstruction in three power system related applications: RLC circuit dynamics, phasor measurement unit (PM) measurements of unknown system, and ac voltage waveform polluted by harmonics. The last application shows that DMD can also replace fast Fourier transformation (FFT) to identify harmonics.**

***Index Terms*—Dynamic mode decomposition, DMD, system identification, power system oscillations.**

I. Introduction

Power system oscillations exist in a grid that has interconnected synchronous generators. Damper windings are installed in units' rotors to reduce the oscillation amplitudes [1]. Oscillations may occur due to sudden events such as faults, outages, or even major load changes. They also lead the system to the same unwanted events. Since they adversely affect the system reliability, they must be addressed and mitigated.

Power system oscillations can be identified by two methods [2]. The first method relies on the system model. Detailed analysis on the dynamic system characteristics, e.g. system state-space and eigenvalues, may reveal the system oscillation modes [3], [1]. Due to the difficulty of modeling real-world power systems, it is practical and faster to implement the second method that provides the possibility identify the model from its measurements. Furthermore, after identifying the system using the data-driven approach, control strategies can be implemented on the identified system to ensure stable operation. Classical ringdown analysis methods in power systems are Prony [4], [5], [2], Matrix Pencil (MP) [6], [5], Eigensystem Realization Algorithm (ERA) [7].

A recent method called Dynamic Mode Decomposition (DMD) has been proposed in fluid field and brain modeling area [8], where it was used to decompose the high-dimensional data into spatial and temporal structures. The DMD algorithm is a combination of several techniques [9]: proper orthogonal decomposition (POD), Fourier transform, Koopman operator, least-square, and singular value decomposition (SVD). Some of the DMD applications are following. First, the DMD has the ability to decompose the spatial and temporal dynamic modes. This advantage of DMD is almost not found in the other model identification methods. The spatiotemporal decomposition yields deep understanding of the transient dynamic behavior. Second, the system dynamical model is constructed based on the dominant spatiotemporal structures. The current system state can be achieved from the dynamical model. Further, the future state may be predicted. Third, since the DMD has the prediction ability, there is a chance of applying control strategies on the system.

978-1-7281-0407-2/19/$31.00 © 2019 IEEE

The scope of this paper is to use DMD to identify the dynamic mode from measurements.

Reference [10] applies DMD under the consideration of setting the given data in pairs of n-dimensional vectors, rather than the time sequential series. In the same reference, the authors compare the DMD with two other system identification techniques that are eigensystem realization algorithm (ERA) and linear inverse modeling (LIM). DMD has been conducted on diverse applications such as fluid experiments [11], foreground/background video separation [12], flows around a high-speed train [13], and financial trading strategies [14].

The first appearance of applying the DMD on power systems is in [15]. The authors exploit the DMD to extract the spatial and temporal modes of inter-area grid oscillations. In [16], DMD is implemented in voltage and frequency measurements of western interconnection.

The aim of this paper is to provide a concise review of DMD algorithm and further demonstrate DMD implementation in power system applications. The first case study of our work is to implement DMD to identify the modes of a simple series RLC circuit. By using sample measurements of the capacitor voltage and the inductor current, modes of the RLC circuit can be identified. Further, distortions are injected to the voltage and current measurements in order that the DMD capability is examined in case the measurements contain noises. In the second case study, PMU power measurements of unknown system are tested on DMD. In these two case studies, the DMD is compared with ERA. Code of ERA has been developed by the USF SPS group [17]. Example code of ERA can also

be found in [18]. The third case study of this paper, voltage measurements that contain undesired components are built to resemble the real-world events. After applying the DMD to the given measurements, it is found able to accurately identify the model and to decompose all the components.

This paper is organized as follows. Section II provides the dynamic mode decomposition background, along with its algorithm details. The DMD in power system implementations are presented in Section III. Section IV concludes the paper.

II. Dynamic Mode Decomposition

This section firstly presents the DMD's general theory, then the DMD's algorithm details.

A. The DMD General Concept

The DMD takes the collected measurements as an input

$$\frac{d\mathbf{x}}{dt} = \mathbf{f}(\mathbf{x}, \mathrm{t}; \mu) \tag{1}$$

where $\mathbf{x}$ is the system state vector, $\mathbf{x} \in \mathbb{R}^n$, at time t. $\mathbf{f}(\cdot)$ is the dynamical continuous-time function, while μ represents the system parameters. Since it is practical to have discrete-time measurements, the discrete-time dynamics is considered

$$\mathbf{x}_{k+1} = \mathbf{F}\left(\mathbf{x}_k\right) \tag{2}$$

where $\mathbf{F}(\cdot)$ is the dynamical discrete-time function. The discrete-state vector $\mathbf{x}_k = \mathbf{x}(k\Delta t)$ for k = 1, 2, ..., m. Δt is the time-sample period, and m is the total number of measurements. If the system is a linear system, (2) can be represented by linear relationship using the dynamics matrix, $\mathbf{A} \in \mathbb{R}^{n\times n}$:

$$\mathbf{x}_{k+1} = \mathbf{A}\mathbf{x}_k. \tag{3}$$

The time-domain expression of $\mathbf{x}(t)$ can be found if the eigenvalues of $\mathbf{A}$ and its eigenvector matrix are known

$$\mathbf{x}(t) = \sum_{k=1}^{n} \boldsymbol{\phi}_k \exp\left(\omega_k t\right) b_k = \boldsymbol{\Phi} \exp(\boldsymbol{\Omega} t)\mathbf{b} \tag{4}$$

where $\boldsymbol{\Omega}$ is a diagonal matrix that contains the continuous-eigenvalues, ω_k, $\boldsymbol{\Phi}$ is the eigenvector matrix, and $\mathbf{b}$ is the coordinates of $\mathbf{x}(0)$ in the eigenvetor basis [9].

The following section presents the DMD algorithm case studies. The DMD framework has the ability to approximate the dynamical system from the system measurement data. The measurements are set in two matrices, one of them has a time shift, in order that the DMD is enabled to approximate the dynamics matrix, $\mathbf{A}$. The measurements matrices:

$$\mathbf{X_1} = \begin{bmatrix} | & | & & | \\ \mathbf{x}_1 & \mathbf{x}_2 & \cdots & \mathbf{x}_{m-1} \\ | & | & & | \end{bmatrix} \tag{5a}$$

$$\mathbf{X_2} = \begin{bmatrix} | & | & & | \\ \mathbf{x}_2 & \mathbf{x}_3 & \cdots & \mathbf{x}_{m} \\ | & | & & | \end{bmatrix} \tag{5b}$$

where $\mathbf{X_1}$, $\mathbf{X_2} \in n \times (m-1)$. This is the standard form of setting the system measurements, which is known as Krylov subspaces. In case of single measurement, the measurement data must be set in a shift-stacking form so that the DMD would be capable of finding the conjugate pair eigenvalues, rather than a single real value [9]. The augmented data matrix form involves both shift-stacking and time-delay, as follows

$$\mathbf{X_{aug,1}} = \begin{bmatrix} x_1 & x_2 & \cdots & x_{m-s} \\ x_2 & x_3 & \cdots & x_{m-s+1} \\ \vdots & \vdots & \ddots & \vdots \\ x_s & x_{s+1} & \cdots & x_{m-1} \end{bmatrix} \tag{6a}$$

$$\mathbf{X_{aug,2}} = \begin{bmatrix} x_2 & x_3 & \cdots & x_{m-s+1} \\ x_3 & x_4 & \cdots & x_{m-s+2} \\ \vdots & \vdots & \ddots & \vdots \\ x_{s+1} & x_{s+2} & \cdots & x_{m} \end{bmatrix} \tag{6b}$$

here, $\mathbf{X_{aug,1}}$, $\mathbf{X_{aug,2}} \in s \times (m-s)$. s represents the time shift, which should be sufficiently large. The data of the case studies of this paper are built in the augmented form as in (6). Although the notation would appear as in (5), the following DMD steps are compatible for both (5) and (6).

Relying on the linear approximation (3) is described in terms of the data measurement matrices, as

$$\mathbf{X_2} \approx \mathbf{A}\mathbf{X_1}. \tag{7}$$

The best-fit dynamics matrix, $\mathbf{A}$, is given by

$$\mathbf{A} = \mathbf{X_2}\mathbf{X_1}^{\dagger} \tag{8}$$

where † denotes the Moore-Penrose pseudoinverse. The system dynamic behavior is model in the dynamics matrix $\mathbf{A}$ from the given measurement data. The DMD algorithm details, which show mode decomposition, system rank, and signal reconstruction, are in the following subsection.

B. The DMD Algorithm

For large-scale systems, evaluating the dynamics matrix, $\mathbf{A}$, could be not only computationally expensive, but intractable. The DMD avoids this complication by using Singular Value Decomposition (SVD). More details and insights on the DMD algorithm can be found in [9]. In this subsection, the algorithm procedure of DMD is briefly described. First, SVD and rank reduction is implemented on $\mathbf{X_1}$:

$$\mathbf{X_1} \approx \mathbf{U}\boldsymbol{\Sigma}\mathbf{V}^*, \tag{9}$$

where $\mathbf{U} \in \mathbb{C}^{n\times r}$, $\boldsymbol{\Sigma} \in \mathbb{C}^{r\times r}$, and $\mathbf{V} \in \mathbb{C}^{m\times r}$, and $*$ refers to the conjugate transpose. $\mathbf{U}$ and $\mathbf{V}$ are unitary matrices, and r is the rank of the SVD approximation. Rank-reduction leads to two advantages: lowering the computation cost and eliminating the noises. In terms of SVD components, (8) becomes

$$\mathbf{A} = \mathbf{X_2}\mathbf{V}\boldsymbol{\Sigma}^{-1}\mathbf{U}^*. \tag{10}$$

The full matrix $\mathbf{A}$ is projected onto the POD modes in order to reduce its rank

$$\tilde{\mathbf{A}} = \mathbf{U}^* \mathbf{A} \mathbf{U} = \mathbf{U}^* \mathbf{X_2} \mathbf{V} \mathbf{\Sigma}^{-1} \tag{11}$$

$\tilde{\mathbf{A}}$ is the reduced-rank dynamics matrix. The lower-rank dynamical model is defined

$$\tilde{\mathbf{x}}_{k+1} = \tilde{\mathbf{A}} \tilde{\mathbf{x}}_k. \tag{12}$$

The full-rank state can be achieved by $\mathbf{x}_k = \mathbf{U}\tilde{\mathbf{x}}_k$. The eigendecomposition is computed on $\tilde{\mathbf{A}}$ so that its eigenvalues and eigenvectors are used to construct the DMD modes and the solution signal.

$$\tilde{\mathbf{A}} \mathbf{W} = \mathbf{W} \mathbf{\Lambda} \tag{13}$$

where $\mathbf{W}$ is eigenvector matrix, and $\mathbf{\Lambda}$ is the eigenvalue diagonal matrix. The eigenvalue corresponds to the discrete-time model. It is converted to the continuous-time model by $\omega_k = \ln(\lambda_k)/\Delta t$.

The DMD exact modes are defined as following

$$\mathbf{\Phi} = \mathbf{X_2} \mathbf{V} \mathbf{\Sigma}^{-1} \mathbf{W}. \tag{14}$$

The initial values of the DMD modes are the components of $\mathbf{b}$ vector. It depends on the initial measurement column vector. The mode initializations

$$\mathbf{b} = \mathbf{\Phi}^{\dagger} \mathbf{x_1}. \tag{15}$$

The signal is reconstructed, thereby the current and the future system continuous-state may be evaluated.

III. The DMD Applications in Power Systems

A. RLC Circuit

1) RLC Base-Case Measurements: In this case study, the DMD is implemented on a series RLC circuit that is shown in Fig. 1. The circuit parameters: V= 1 volt, Δt= 0.001 s, R= 1 Ω, L= 0.01 H, and C= 0.001 μ. The dynamics matrix, $\mathbf{A}$, with inductor current i_L and the capacitor voltage v_C as state variables, is defined as follows.

$$\mathbf{A} = \begin{bmatrix} \frac{-R}{L} & \frac{-1}{L} \\ \frac{1}{C} & 0 \end{bmatrix} = \begin{bmatrix} -100 & -100 \\ 1000 & 0 \end{bmatrix}.$$

Since the RLC circuit is a second order system, it has two eigenvalues, $\lambda_{1,2}$, that are $-50.00 \pm j312.25$. A step change is given in the source voltage and the dynamic system is simulated via MATLAB function `lsim` [19]. The RLC solution for 0.1 s, taking into account the sampling rate of 0.001 s, consists of 100 signal points. The capacitor voltage and the inductor current measurement samples are used as DMD input. Only the first 20 points of the solution are employed. The measurement time shift, s, is chosen to be 10. The size of both $\mathbf{X_{aug,1}}$ and $\mathbf{X_{aug,2}}$ is (20×10). It should be noted that the rows of the data matrices are 20, twice s, bearing in mind that the DMD input is comprised

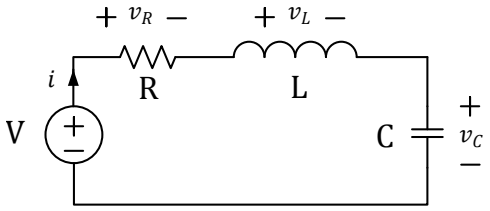

Fig. 1. Series RLC circuit.

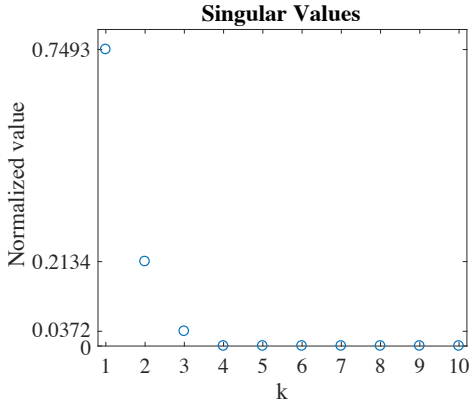

Fig. 2. RLC case study singular values.

of two signals. Even though $\mathbf{X_{aug,1}}$ rank is 10, the rank-reduction is primarily based on the effective singular values, from the diagonal matrix $\mathbf{\Sigma}$. This case has three non-zero effective singular values that have most the data information. The rest of the ineffective singular value can be disregarded. The normalized singular values are plotted in Fig. 2. Therefore, the DMD rank, r, is 3. Consequently, the rank-reduction of this case helps to circumvent 70 % of unnecessary computation.

The DMD solution is compared with the ERA method as well as the original model. The reconstructed signals are shown in Fig. 3, whereas the eigenvalues are plotted in Fig. 4. It can be seen that both methods exactly match the original system.

2) RLC Measurements with 10% Noises: Since the measurements of the real world inherently contain noises, 10% random noises are added to the measurement signals. The purpose of this case study is to inspect both DMD and ERA methods with noises. In this case, the system rank is chosen as 3 based on the effective singular values. The DMD and ERA model identification solutions are shown in Fig. 5. Because the model eigenvalues with 10% noises are not known, we compare the DMD and ERA eigenvalues with each other. They are found in Fig. 6. It can be seen that while the ERA eigenvalues slightly change, the DMD eigenvalues stand still and match the original model.

B. PMU Measurements

The DMD and ERA algorithms are implemented on PMU data of power measurements during an oscillatory event, taken from [20]. The data are shown in Fig. 8. The data-set records

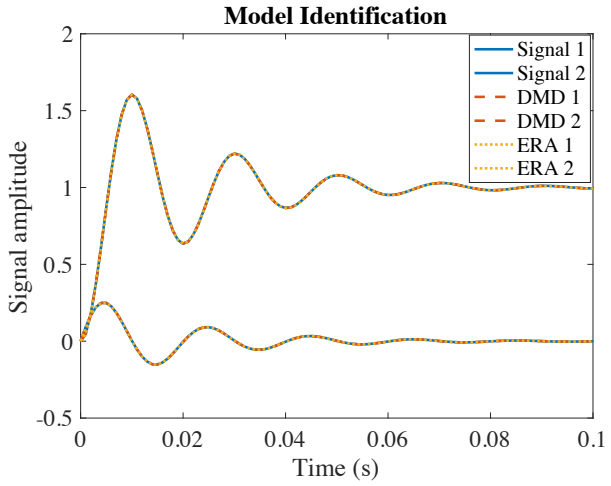

Fig. 3. Base-case model along with DMD and ERA model identifications.

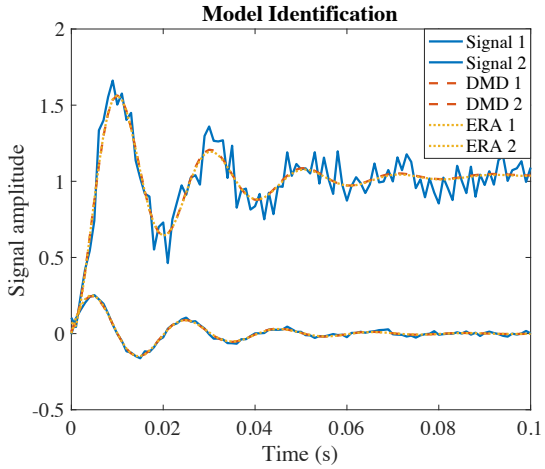

Fig. 5. The 10% noisy measurements along with DMD and ERA model identification.

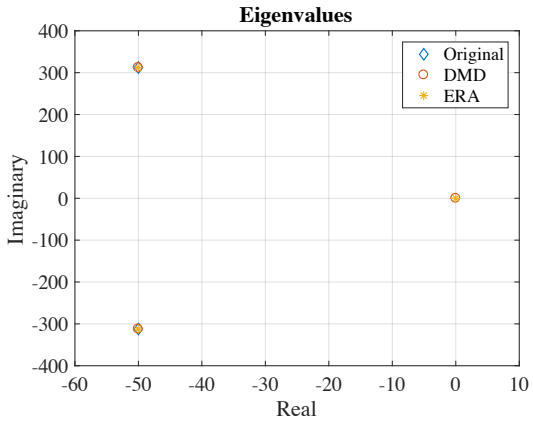

Fig. 4. Base-case model, DMD, and ERA eigenvalues.

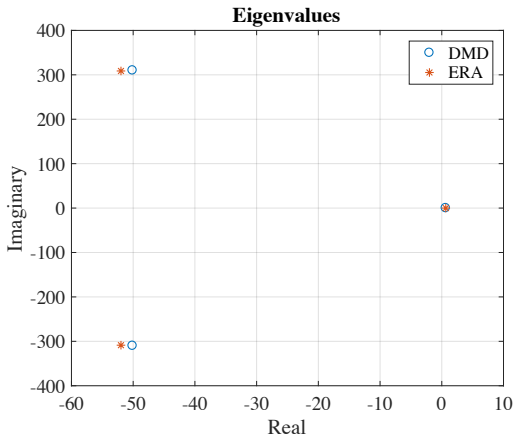

Fig. 6. The DMD and ERA eigenvalues of 10% noisy measurements.

15 s, with sampling rate of 0.05 s, after the event occurrence in the grid. The measured signal points are 301, and they are plugged in the DMD. s, the time shift, is selected to be 150, so the size of $\mathbf{X_{aug,1}}$ and $\mathbf{X_{aug,2}}$ is (150×151). Due to lack of information of the measured system, the system order can be estimated by considering the most effective singular values. The normalized singular values for this case are drawn in Fig. 7. Since the measurement contains noises, and our goal is to express the system without noises, the DMD rank is chosen to be the number of the most dominant singular values, which is 5. The DMD rank can be higher, but this adds ripples and meaningless eigenvalues to the identified model. Furthermore, if rank-reduction is not performed, all the singular values are included, the DMD fails to identify the model. The original measurements along with the DMD and the ERA identification are shown in Fig. 8. The DMD and ERA eigenvalues are found in Fig. 9. The identified eigenvalues of both methods are comparable.

C. Abnormal Operation Analysis

The distribution-level system typically has unbalanced and harmonic components. Moreover, faults and sudden disturbances add tremendous distortions to the network. Since these undesired electrical components greatly harm both the grid and the consumers' devices, a detailed analysis must be performed to track the disturbance issues. As an example, if the voltage has a second-order harmonic and a fifth-order harmonic components, the phase "a" voltage is represented as follows.

$$V_{sa}(t) = \widehat{V}_s \cos(\omega_0 t) + k_2 \widehat{V}_s \cos(2\omega_0 t) + k_5 \widehat{V}_s \cos(5\omega_0 t)$$

where $\widehat{V}_s$ is the voltage peak magnitude. The second-order and fifth-order harmonic components are k_2 and k_5, respectively. t represents time, whereas the system radian frequency is ω_0. The DMD algorithm is applied on the given data as if we do not know the original system. This reverse engineering technique demonstrates the DMD ingenuity.

The values of this example are $\widehat{V}_s = 1$, $k_2 = 0.1$, $k_5 = 0.25$, and $\omega_0 = 2\pi 60$. The voltage data and also the DMD

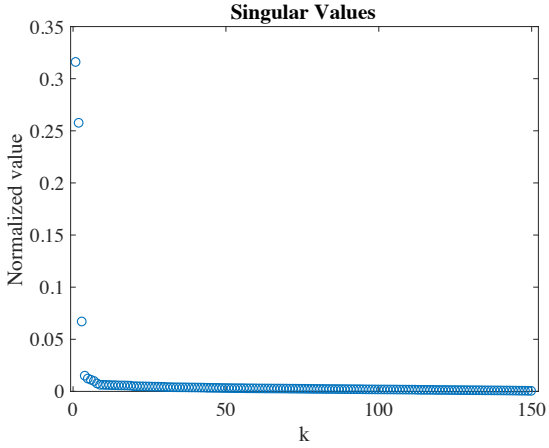

Fig. 7. Singular values of PMU measurements.

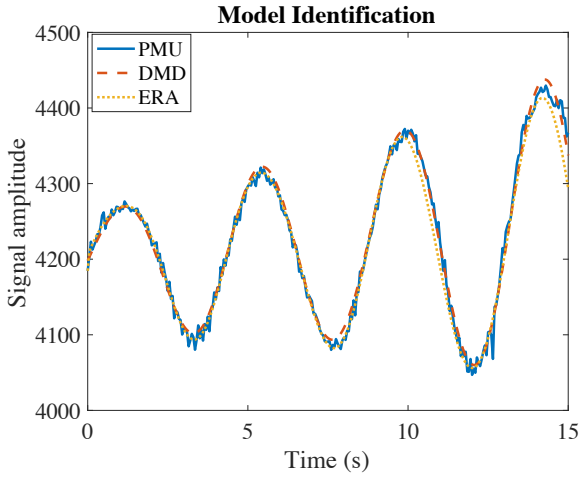

Fig. 8. The PMU measurements together with the DMD and ERA model identification.

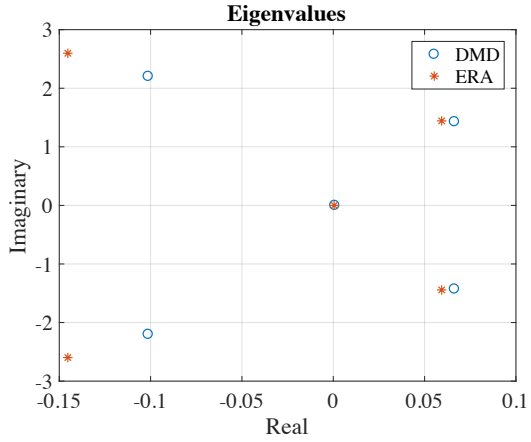

Fig. 9. The DMD and ERA eigenvalues of the PMU measurements.

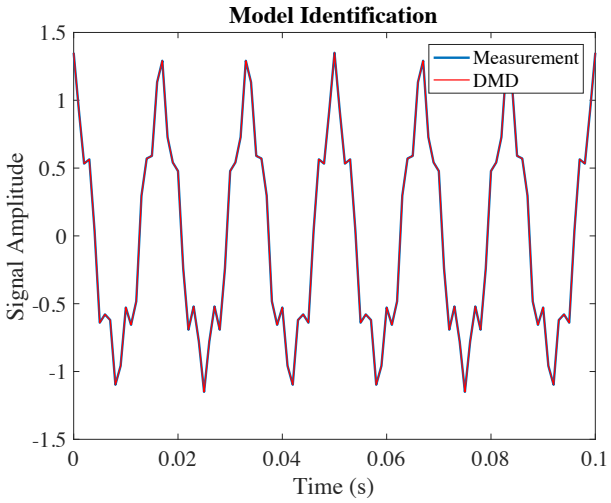

Fig. 10. $V_{sa}(t)$ original data and the DMD identification.

identification are drawn Fig. 10, which appear distorted.

The voltage data-set duration is 0.1 s with sampling rate of 0.001 s. So, the input signal constructed of 101 samples. s is selected to be 50, that is, the size of $\mathbf{X_{aug,1}}$ and $\mathbf{X_{aug,2}}$ is (50×51). The singular values of this case are shown in Fig. 11. The effective singular values are 6, as expected since each cosine has two eigenvalues. Thus, the DMD rank is 6. DMD builds the system of which its eigenvalues are plotted Fig. 12. The DMD gives the ability to decompose the given signal, the modes are found in Fig. 13. Mode 1, mode 2, and mode 3 are associated with fundamental, fifth-harmonic, and 2nd harmonic components, respectively. The DMD arranges the signal modes in dominance order. Each mode's coefficient is also identified by b. The coefficients against the fundamental component's coefficient are shown in Fig. 14. The results exactly match the given coefficients.

From this analysis, operational engineers have a closer look to the measured signal from which they can easily know all the system details and fix it. For instance, the given case study is found to contain second and fifth-order harmonic components.

IV. Conclusion

The dynamic mode decomposition algorithm has been found very useful in many engineering areas. The authors of this paper motivate the use of the DMD in power system applications. Besides of the DMD high accuracy of identifying a model, it has the capability to decompose the system dynamic modes. The first case study shows the DMD ability to identify the RLC circuit modes from a few measurement samples. DMD is found to be as good as ERA. Then, we intentionally add noises to the RLC measurements to examine both methods, and it is noticed that the DMD is more robust because its eigenvalues remain unchanged as in the base case. In the second case study, the DMD is applied on PMU power measurement data of an unknown system. The solution is found comparable to the ERA method. In the third case study, the data-set represents voltage measurement that is distorted due to disturbance, and the DMD is capable to identify all the measurement component details.

References

[1] G. Rogers, *Power system oscillations*. Springer Science & Business Media, 2012.

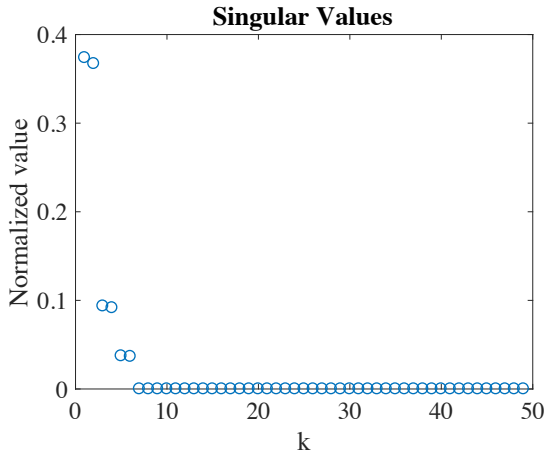

Fig. 11. Voltage measurement singular values.

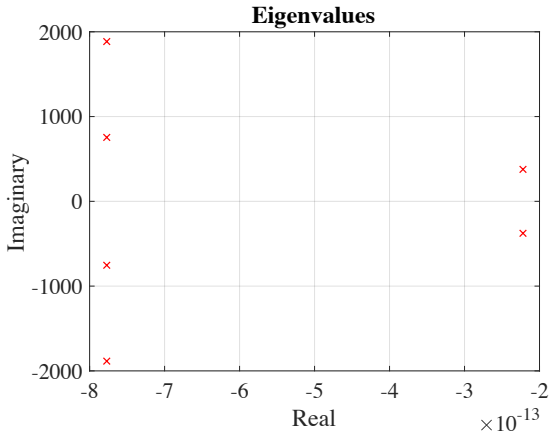

Fig. 12. $V_{sa}(t)$ data eigenvalues from DMD.

[2] L. Fan, "Data fusion-based distributed prony analysis," *Electric Power Systems Research*, vol. 143, pp. 634–642, 2017.

[3] ——, "Interarea oscillations revisited," *IEEE Transactions on Power Systems*, vol. 32, no. 2, pp. 1585–1586, 2017.

[4] J. F. Hauer, C. Demeure, and L. Scharf, "Initial results in prony analysis of power system response signals," *IEEE Transactions on power systems*, vol. 5, no. 1, pp. 80–89, 1990.

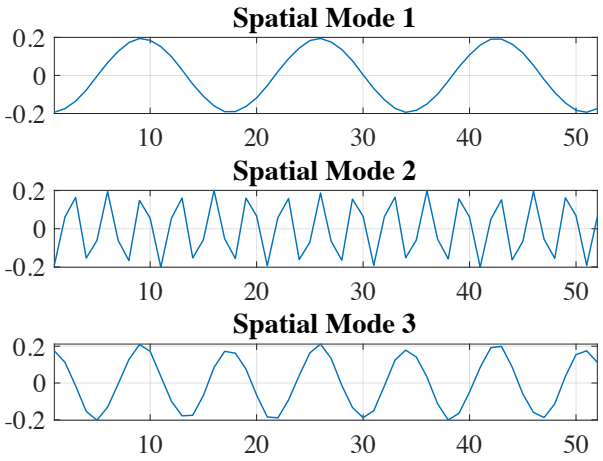

Fig. 13. $V_{sa}(t)$ modes.

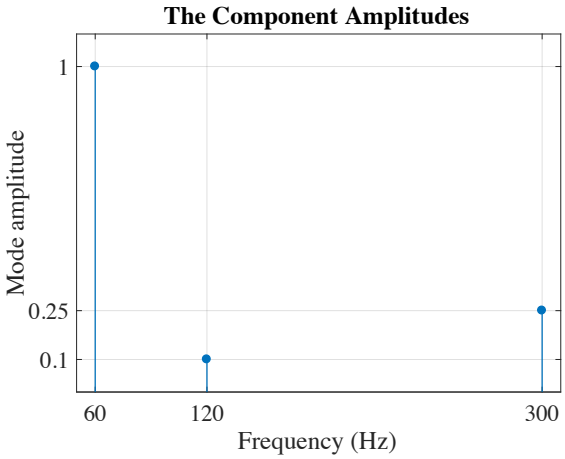

Fig. 14. $V_{sa}(t)$ mode factors.

[5] L. L. Grant and M. L. Crow, "Comparison of matrix pencil and prony methods for power system modal analysis of noisy signals," in *2011 North American Power Symposium*. IEEE, 2011, pp. 1–7.

[6] Y. Hua and T. K. Sarkar, "Matrix pencil method for estimating parameters of exponentially damped/undamped sinusoids in noise," *IEEE Transactions on Acoustics, Speech, and Signal Processing*, vol. 38, no. 5, pp. 814–824, 1990.

[7] J. Sanchez-Gasca, "Computation of turbine-generator subsynchronous torsional modes from measured data using the eigensystem realization algorithm," in *2001 IEEE Power Engineering Society Winter Meeting. Conference Proceedings (Cat. No. 01CH37194)*, vol. 3. IEEE, 2001, pp. 1272–1276.

[8] P. J. Schmid, "Dynamic mode decomposition of numerical and experimental data," *Journal of fluid mechanics*, vol. 656, pp. 5–28, 2010.

[9] J. N. Kutz, S. L. Brunton, B. W. Brunton, and J. L. Proctor, *Dynamic mode decomposition: data-driven modeling of complex systems*. SIAM, 2016.

[10] J. H. Tu, C. W. Rowley, D. M. Luchtenburg, S. L. Brunton, and J. N. Kutz, "On dynamic mode decomposition: theory and applications," *arXiv preprint arXiv:1312.0041*, 2013.

[11] P. J. Schmid, "Application of the dynamic mode decomposition to experimental data," *Experiments in fluids*, vol. 50, no. 4, pp. 1123–1130, 2011.

[12] J. Grosek and J. N. Kutz, "Dynamic mode decomposition for real-time background/foreground separation in video," *arXiv preprint arXiv:1404.7592*, 2014.

[13] T. W. Muld, G. Efraimsson, and D. S. Henningson, "Flow structures around a high-speed train extracted using proper orthogonal decomposition and dynamic mode decomposition," *Computers & Fluids*, vol. 57, pp. 87–97, 2012.

[14] J. Mann and J. N. Kutz, "Dynamic mode decomposition for financial trading strategies," *Quantitative Finance*, vol. 16, no. 11, pp. 1643–1655, 2016.

[15] E. Barocio, B. C. Pal, N. F. Thornhill, and A. R. Messina, "A dynamic mode decomposition framework for global power system oscillation analysis," *IEEE Transactions on Power Systems*, vol. 30, no. 6, pp. 2902–2912, 2015.

[16] S. Mohapatra and T. J. Overbye, "Fast modal identification, monitoring, and visualization for large-scale power systems using dynamic mode decomposition," in *2016 Power Systems Computation Conference (PSCC)*. IEEE, 2016, pp. 1–7.

[17] A. Almunif and L. Fan, "A tutorial on data-driven eigenvalue identification: Prony analysis, matrix pencil and eigensystem realization algorithm," *submitted, Electric Power Systems Research*.

[18] S. L. Brunton and J. N. Kutz, *Data Driven Science & Engineering: Machine Learning, Dynamical Systems, and Control*. Cambridge University Press, 2019.

[19] L. Fan, *Control and dynamics in power systems and microgrids*. CRC Press, 2017.

[20] P. W. Sauer, M. A. Pai, and J. H. Chow, *Power system dynamics and stability: with synchrophasor measurement and power system toolbox*. John Wiley & Sons, 2017.